JMEPEG (2004) 13:172-184
DOI: 10.1361/10599490418451

1059-9495/$19.00

The Effect of Globular Microstructure Size on the Mechanical Properties in Reheating Process of Aluminum Alloys

C.G. Kang, S.W. Youn, and P.K. Seo

(Submitted 9 August 2002; in revised form 24 February 2003)

One of the important steps in semi-solid forming is the process of reheating raw materials to the semi-solid state. This process is not only necessary to achieve the required semi-solid state of the billet, but also to control the microstructure of the billet. In the reheating process, the globule size is determined by the holding time of the final reheating step. Therefore, some experiments to investigate the relationship between the mechanical properties and the holding time in the last heating step were performed. The alloys used in this experiment were 357, 319, and A390 alloys. The experiments of reheating were performed using an induction heating system with a capacity of 50 kW. This article shows the evolution of the microstructure according to the holding time of the last reheating stage. Furthermore, to evaluate the effect of globule size as determined by holding time of the final reheating step, uniaxial tension tests were performed. The stress-strain curves were plotted according to the holding time, and a relationship between the microstructure and the flow stress of semi-solid material was formulated.

Keywords globule size, holding time, mechanical property, reheating, semi-solid forming

1. Introduction

The thixoforging process can be used to fill a die cavity at lower loads and at lower temperatures than either squeeze casting or die-casting.[1-4] In addition, thixoforging can reduce casting defects due to lower gas content. As a result of these advantages, its application to the manufacture of automotive and compact electronic parts has been actively pursued.

The induction heating process is very important in the thixoforging process. Not only is the induction heating process necessary to achieve the required semi-solid billet state, but also to control the microstructure of the billet. The main objective of the reheating process is to reheat the billet to the desired temperature. However, the microstructure of the semi-solid material can be controlled by changing the reheating process parameters, such as the reheating temperature, reheating time, and holding time, during the reheating process. Due to the importance of the reheating process, many studies investigating the proper reheating conditions have been actively carried out.[5-7]

Among the factors that strongly affect the mechanical properties of the semi-solid processed component, the solid fraction, the level of the globularization, the globular microstructure size and distribution, the Si distribution within eutectic, and the temperature distribution can be controlled during the reheating process.

From this point of view, Lou et al.[8] have studied the relationship between the aspect ratio and size variation of the globular microstructure for variation of the holding time of the reheating temperature through reheating experiments using A356 and A357 alloys. Sannes et al.[9] have studied the distribution and the size of the globular microstructure of an Mg alloy with variations in the holding time of the reheating temperature. Wang et al.[10] have investigated the solid grain size change of an Al-80%Zn alloy with variation in solid fraction. Ferrante and de Fretias[11] have investigated that the microstructure change of an Al-4 wt.%Cu alloy with variations in the holding time of the reheating temperature. Jung and Kang[12] have reported microstructures of A356 aluminum (Al) alloy with a variety of reheating times and temperatures.

Up to now, most studies that have been performed were focused mainly on the investigation of the microstructural change with variation of the holding time of the reheating process. However, studies on the relationship between the mechanical properties and microstructure are very limited.

Also, for analysis of the thixoforming process, it is necessary to formulate stress-strain curves for semi-solid alloys. However, the number of studies on the relationship between microstructure and mechanical properties that can be used for strength analysis of the thixoformed components are very limited.

Therefore, to establish the quantitative relationship between the microstructure and the mechanical properties, thixoforged components with variations in the reheating conditions were investigated. The change in the globular microstructure size was investigated as a function of the holding time of the final step (t_{h3}) in the reheating process. Tensile tests were performed to investigate the effect of the globular size on mechanical properties. Also, for application to the semi-solid material com-

C.G. Kang, Engineering Research Center for Net Shape and Die Manufacturing (ERC/NSDM), School of Mechanical Engineering, Pusan National University, Pusan 609-735, South Korea; and **S.W. Youn** and **P.K. Seo,** Department of Mechanical and Precision Engineering, Graduate School of Pusan National University, Pusan 609-735, South Korea. Contact e-mail: cgkang@pusan.ac.kr.

Table 1 Chemical Compositions of Aluminum Alloys

Specimen	Composition	Si	Fe	Cu	Mn	Mg	Ni	Zn	Ti	Pb
357	Min(%)	6.5	…	…	…	0.50	…	…	…	…
	Max(%)	7.5	0.15	0.03	0.03	0.60	0.03	0.05	0.20	0.03
319	Min(%)	5.5	…	2.5	…	0.3	…	…	…	…
	Max(%)	6.5	0.15	3.5	0.03	0.4	0.03	0.05	0.20	0.3
A390	Min(%)	16.0	…	4.0	…	0.5	…	…	…	…
	Max(%)	17.0	0.4	5.0	0.1	0.65	0.01	0.05	0.20	0.03

Table 2 Reheating Condition of Aluminum Alloys

	Heating Time, min			Heating Temperature, °C			Holding Time, min					
Material	t_{a1}	t_{a2}	t_{a3}	T_{h1}	T_{h2}	T_{h3}	t_{h1}	t_{h2}	t_{h3}	t_{h3}	t_{h3}	t_{h3}
357	3	2	2	375	576	583	1	1	1	2	3	4
319	4	2	2	450	560	578	1	1	1	2	3	4
A390	4	2	2	450	560	570	1	1	1	2	3	4

ponent fabrication, the size change of the globular microstructure with variation in the holding time of the final reheating temperature (t_{h3}) was quantified by image analysis.

The materials used in this study were 319 and A390 alloys, having good strength and wear resistance, respectively, as well as 357 alloy that is commonly used in semi-solid processing.

2. Experimental Procedure

2.1 Reheating Process

The materials used in this study were hypoeutectic Al-Si7Mg (357) and Al-Si6Cu3Mg (319) alloys, and a hypereutectic Al-Si17Cu4Mg alloy (A390), which were fabricated by linear electromagnetic stirring by Pechiney (France). Chemical compositions of Al alloys are listed in Table 1.

During induction heating, the relationship between time and temperature must be controlled exactly to obtain a uniform temperature distribution over the entire cross-sectional area of the billet. In this study, for the reheating experiments, an induction heating system with a capacity of 50 kW was used to reduce the total reheating time and to control the billet temperature accurately. The temperature of the alloys was measured at three positions by using K-type chromel-alumel thermocouples that were 1.6 mm in diameter. The dimensions of the specimens and the temperature measuring positions are shown in Fig. 1. During the reheating step, the control of the billet temperature was performed according to the temperature at position B in Fig. 1.

In the reheating process, control of the billet temperature was carried in one of two ways. In the first method, the temperature of the billet is measured and controlled directly using a thermocouple. In this case, it is possible to control the billet temperature accurately because the induction-heating capacity needed to reheat the billet is calculated in real time during the reheating process. However, this method is not feasible for use in the mass production of the semi-solid component because a thermocouple must be inserted into the billet.

In the second method, the billet temperature is controlled according to the preset temperature profile. In this method, a thermocouple is not necessary, so it is feasible for use in the mass production of the semi-solid component. However, the variation in the temperature profile with material type and billet size must be investigated, and the accuracy of the temperature control is lower than in the first method. In the current study, the first temperature control method was used to control the billet temperature.

To obtain the fine globular microstructure, the eutectic must be melted completely, and the reheating time must allow for complete eutectic melting. Before and after the melting of the eutectic, the solid fraction changes rapidly, and a rapid temperature rise occurs when the eutectic is melted. Due to this temperature rise, controlling the reheating temperature is difficult. Therefore, to achieve a homogeneous temperature distribution and a consistent solid fraction of the billet in the semi-solid state, the billet was reheated in three steps.[12,13] The reheating conditions used in this study are listed in Table 2. To obtain a proper solid fraction of 55%, and to achieve the homogeneous distribution of globular microstructures while reducing material loss, reheating experiments were performed for variations of the holding time during the final step (t_{h3}).

2.2 Evolution of Microstructure

To quantify the globularization of the microstructure, the mean equivalent diameter ($D_{eq.}$) and roundness (R) of microstructure were measured using image analysis techniques. An equivalent diameter is the diameter of a circle having the same area as the globular structure, and this is represented by Eq 1, where A is the area of the globular feature,

$$D_{eq} = \sqrt{\frac{4A}{\pi}} \qquad \text{(Eq 1)}$$

R is a dimensionless shape factor describing the circularity of a feature and is represented by Eq 2.

$$R = \sqrt{\frac{p^2}{4\pi A}} \qquad \text{(Eq 2)}$$

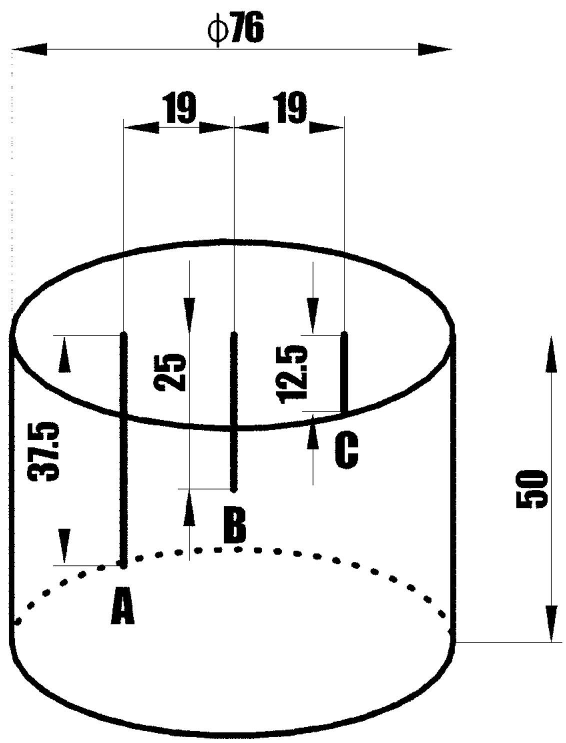

Fig. 1 Billet size and temperature measuring point (in millimeters)

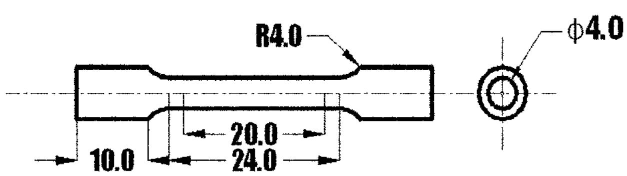

Fig. 2 Tensile test specimen (in millimeters)

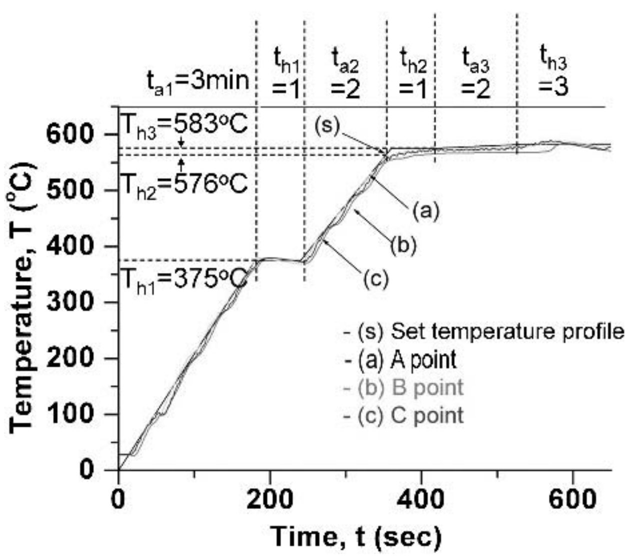

Fig. 3 Temperature profile during reheating process of 357 alloy

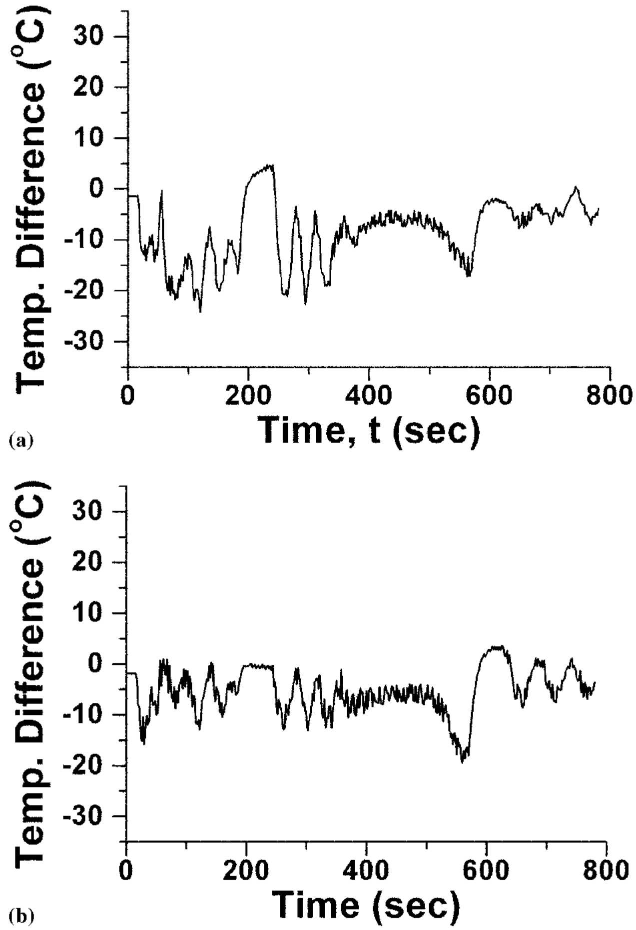

Fig. 4 Temperature difference during the reheating process of the 357 alloy: **(a)** between points A and B; and **(b)** between points B and C

Here, p and A are the perimeter and the area of the solid grain, respectively. A true circle would have a roundness of one. All other objects have roundness values greater than one.

2.3 Tension Tests

For tension tests at room temperature, a round tensile test specimen (ASTM E 8M) with 20 mm gage length and 4 mm diameter was used, as shown in Fig. 2. A strain rate of 0.5×10^{-3} s^{-1} was used, and an extensometer was attached to the specimen to record accurate elongation data. Stress and strain values were obtained from the data, and a 0.2% offset yield stress was calculated. To formulate the relationship between solid grain size and stress-strain relation, the strength coefficient (K) and the strain-hardening exponent (m) were calculated.

3. Experimental Results and Discussions

3.1 Reheating Experiment

3.1.1 Temperature Difference Over the Diameter of the Billet During Reheating. Figure 3 shows the time-

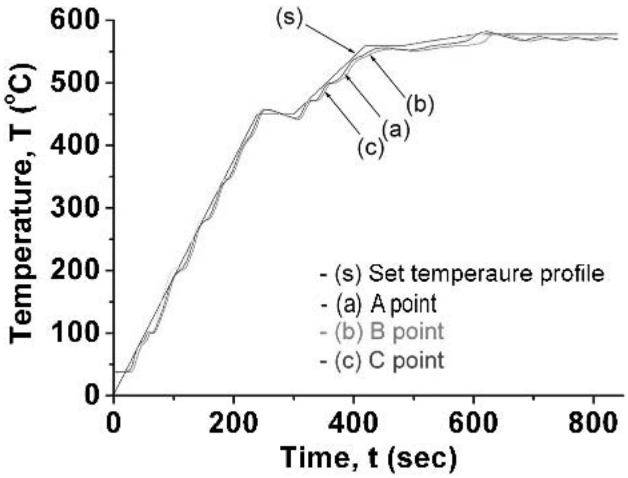

Fig. 5 Temperature profile during reheating process of 319 alloy

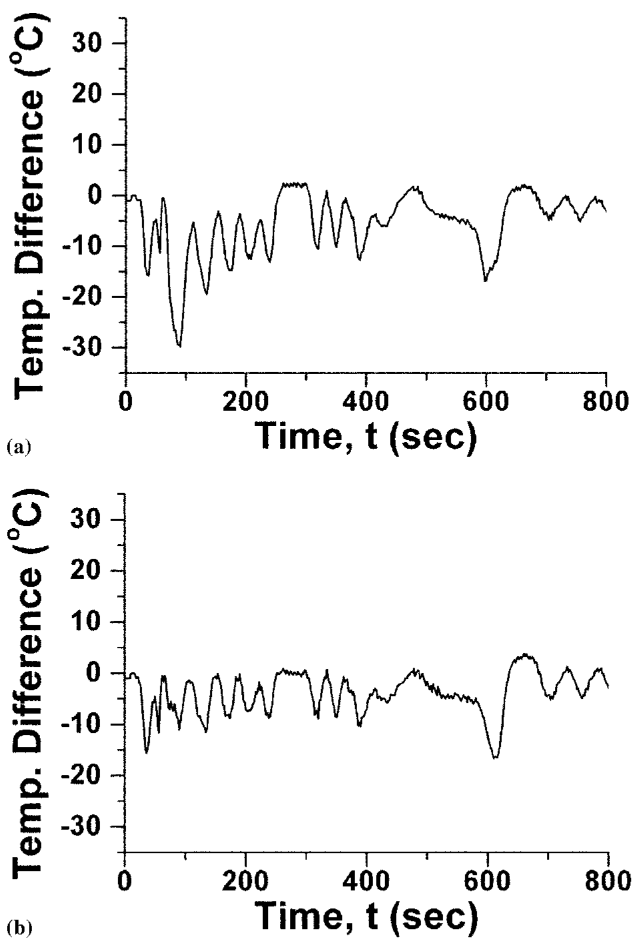

Fig. 6 Temperature difference during reheating process of 319 alloy: **(a)** between points A and B; and **(b)** between points B and C

temperature curve of the 357 Al alloy that was recorded during reheating. It is known that the billet was reheated to the desired temperature according to the temperature profile.

In common induction heating systems, the induced heat is

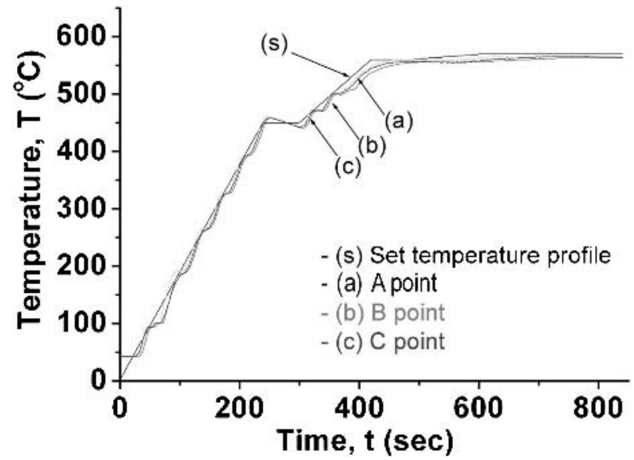

Fig. 7 Temperature profile during reheating process of A390 alloy

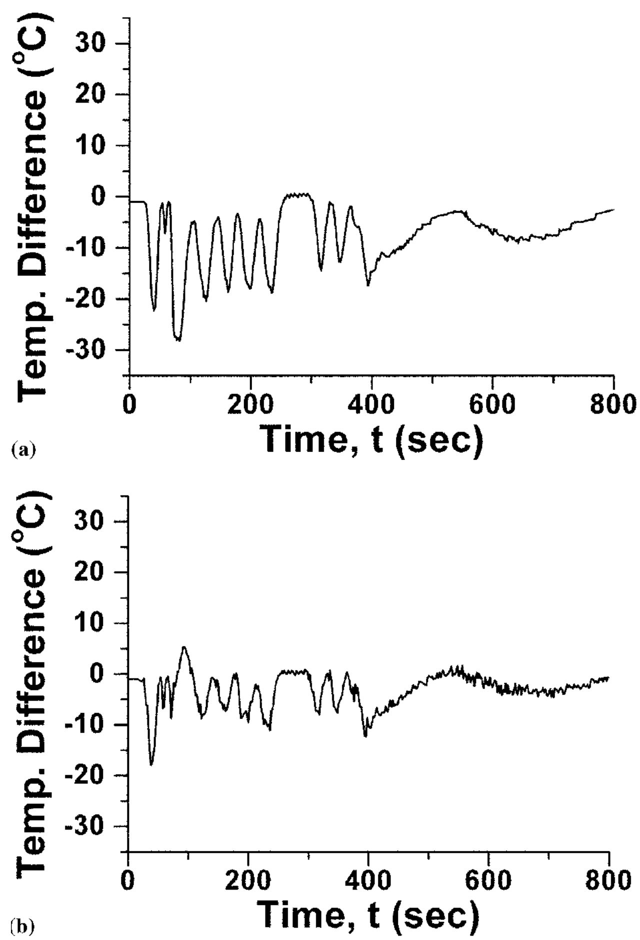

Fig. 8 Temperature difference during reheating process of A390 alloy: **(a)** between points A and B; and **(b)** between points B and C

normally not equally distributed over the entire length of the billet. Due to the skin effect, approximately 86% of the power is concentrated within a surface layer of the inductively heated billet.[14] Therefore, to obtain a homogeneous temperature distribution over the diameter of the billet, holding time was set at

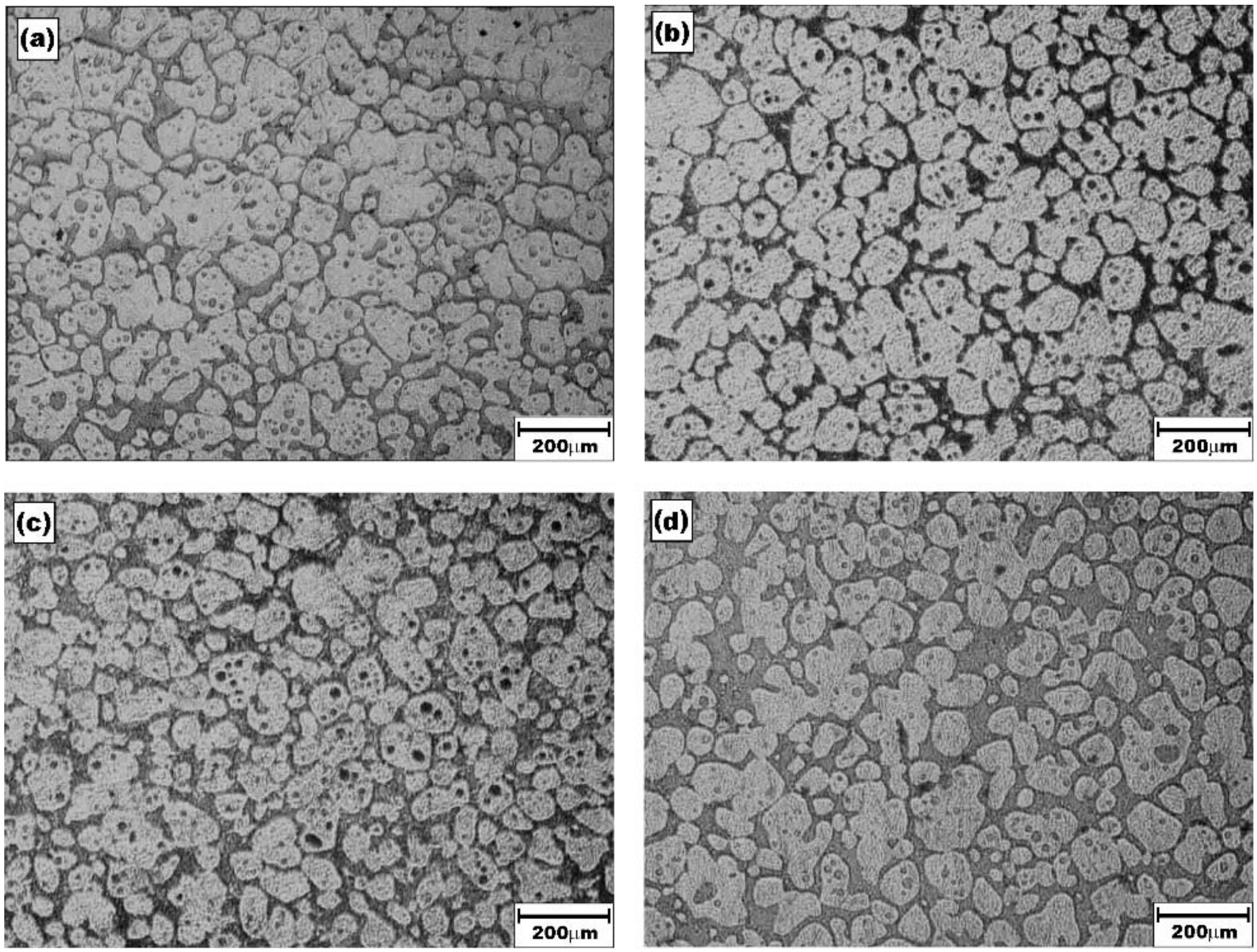

Fig. 9 Microstructure evolution of the 357 alloy with variation in the t_{h3}: **(a)** 1 min; **(b)** 2 min; **(c)** 3 min; and **(d)** 4 min

each reheating step. During the holding step, the temperature profile of the billet is mainly dominated by conduction rather than the induction heating capacity, because the induction heating capacity during the holding step is much lower than that during heating step. Therefore, the temperature difference between the center and the edge of the billet was reduced during the temperature holding step.

Figure 4(a,b) show the temperature differences between thermocouple positions A-B and between B-C in Fig. 1. In the first step of billet reheating, the temperature difference is approximately 25 °C but has improved during the holding step at the reheating temperature. It was observed that the temperature difference of the final reheating step is reduced to approximately 0 °C.

Figures 5-8 show the temperature differences between the 319 and A390 alloys during reheating process. Similar to the case with the 357 alloy, the temperature difference in the final step was reduced to 0 °C.

3.1.2 Microstructural Change With Variation in the Holding Time of the Final Reheating Step (t_{h3}). The microstructural changes associated with the holding time of the final step (t_{h3}) were observed. The holding time during the final step (t_{h3}) was varied between 1 and 4 min.

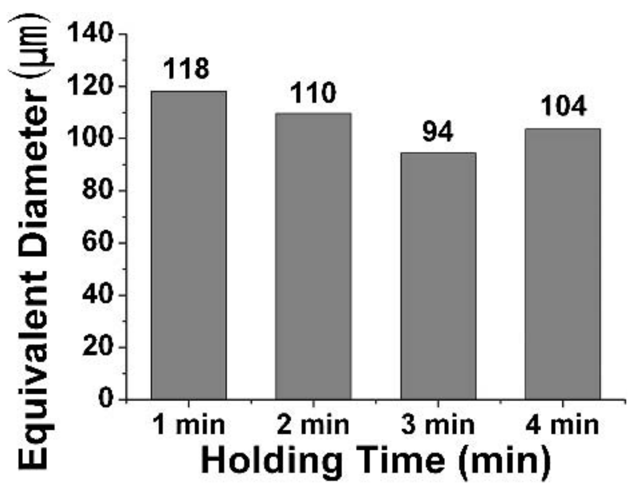

Fig. 10 Globule size of the 357 alloy with variation in the t_{h3}

Figure 9 shows the influence of final holding time (i.e., t_{h3} = 1, 2, 3, and 4 min) during reheating on the microstructure of the 357 alloy. It was observed that the globularization of the

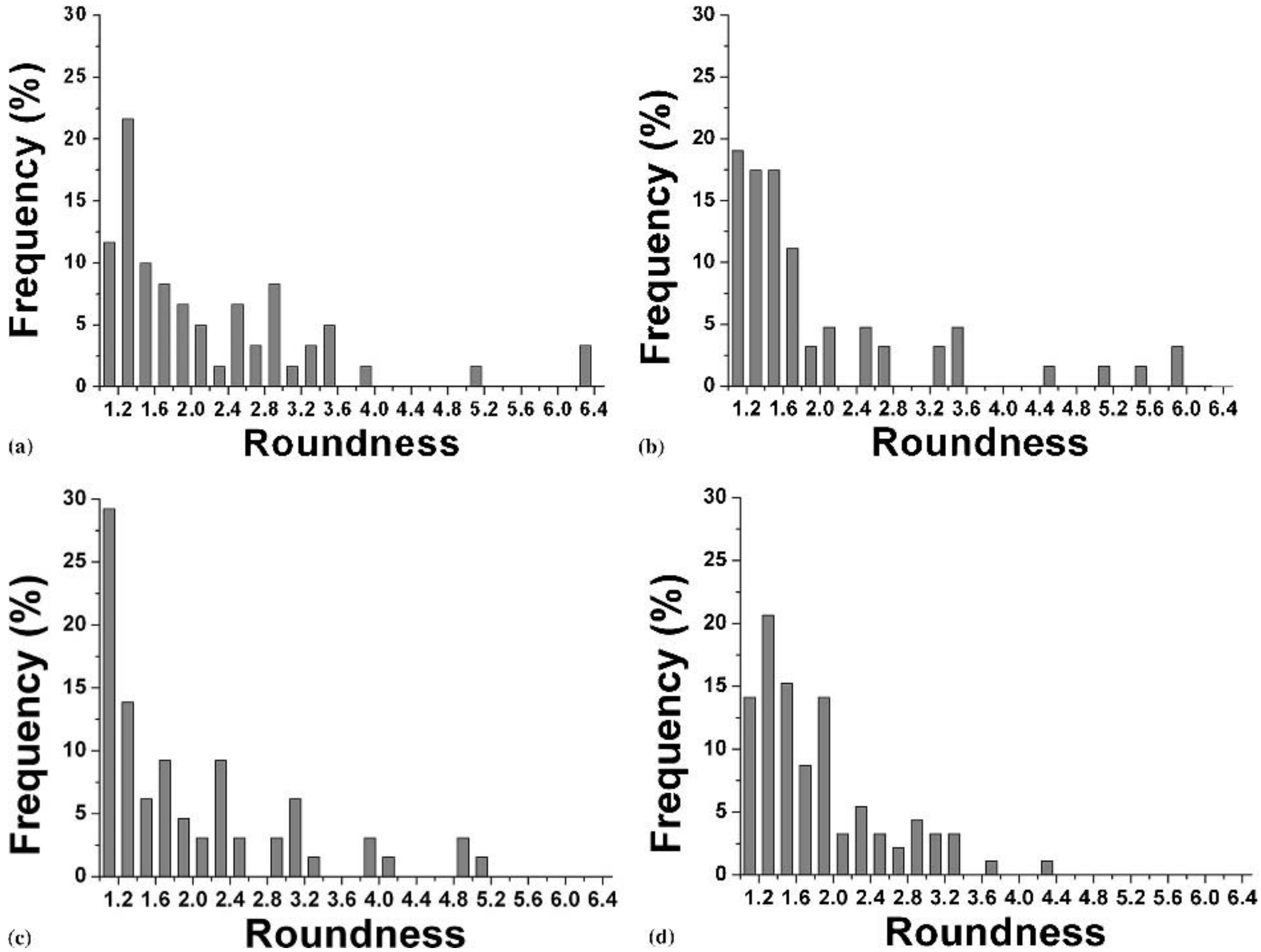

Fig. 11 Roundness of 357 with variation in the t_{h3}: **(a)** $t_{h3} = 1$ min; **(b)** $t_{h3} = 2$ min; **(c)** $t_{h3} = 3$ min; and **(d)** $t_{h3} = 4$ min

microstructure increased with increasing t_{h3}. However, when t_{h3} was longer than 4 min, coarsening of the solid grain was observed. To quantify the globular microstructure size, a mean equivalent diameter of the solid grains was measured using image analysis.

Figure 10 shows the mean equivalent diameter of the 357 alloy with variations in the holding time of the final reheating temperature (t_{h3}). A minimum mean equivalent diameter of the solid grains of 94 μm was obtained for a reheating condition of $t_{h3} = 3$ min. If the holding time of the final step (t_{h3}) is shorter than 3 min, sufficiently globularized solid grains are not obtained due to the lack of the time for solid grain growth. On the other hand, if the holding time (t_{h3}) is longer than 3 min, the microstructures become coarse due to the growth and coalescence of solid grains.[10]

Figure 11 shows the R distributions for the 357 alloys with variation of the holding time of the final step (t_{h3}). In the case of $t_{h3} = 1$ min, a percentage of the solid grains with $1 \le R \le 1.2$ and $1 \le R \le 2$ were 11.7% and 58.3%, respectively. In the case of $t_{h3} = 2$ min, a percentage of the solid grains with $1 \le R \le 1.2$ and $1 \le R \le 2$ were 19.0% and 68.3%, respectively. It was observed that the level of the globularization of the microstructure increases remarkably in the t_{h3} range of 1-2 min. In case of $t_{h3} = 3$ min, the volume fraction of solid grains with $1 \le R \le 1.2$ is 14.1%. This value is relatively lower than the case of the $t_{h3} = 2$ min, but the volume fraction of solid grains ($1 \le R \le 2$) is the highest at 72.8%. In the case of $t_{h3} = 4$ min, the volume fraction of the solid grain with $1 \le R \le 1.2$ has the highest value at 29.2%, but that with $1 \le R \le 2$ was reduced to 63.1% due to the solid grain coarsening and coalescence effects. From these data, it was found that $t_{h3} = 3$ min is the best reheating condition for obtaining the globular microstructure.

Figure 12 shows the microstructure of the 319 Al alloy with variations in the holding time of the final reheating step (t_{h3}). In the case of $t_{h3} = 1$ min, the globular microstructures were not obtained due to the lack of sufficient holding time for the separation of solid and liquid, before and after the phase change.

When the holding time of the final reheating step (t_{h3}) is 3 min, it was observed that the fine and globular solid grains were well distributed. In the case of $t_{h3} = 4$ min, more globular microstructures were obtained than in the case of $t_{h3} = 3$ min, but there was some gradient in terms of the microstructure size. To quantitatively investigate the effect of the holding time of the final step (t_{h3}) on globular microstructure, an equivalent diameter of solid grain was measured using the image analysis system.

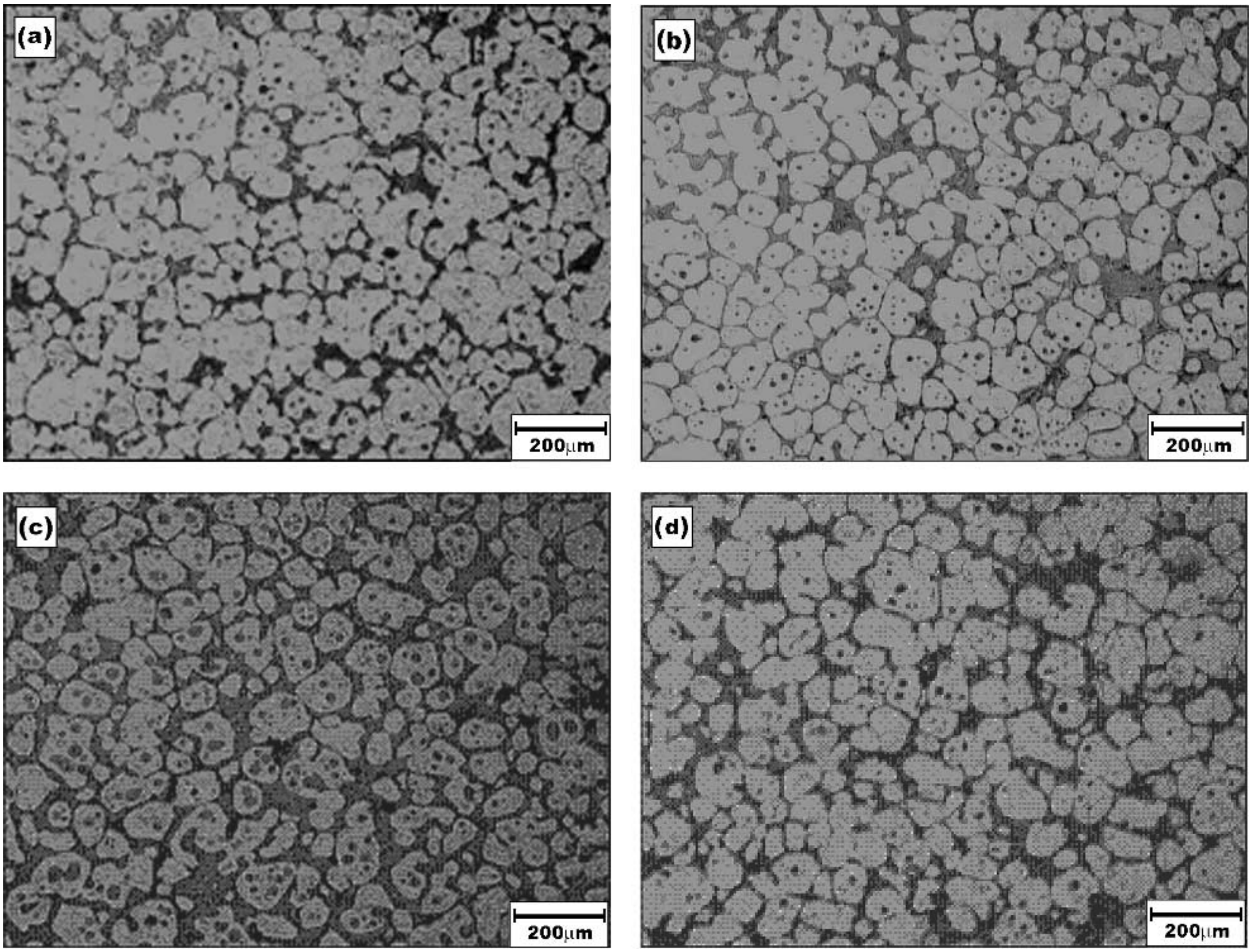

Fig. 12 Microstructure evolution of the 319 alloy with variation in the t_{h3} of **(a)** 1 min, **(b)** 2 min, **(c)** 3 min, and **(d)** 4 min

Figure 13 shows the mean equivalent diameter (D_{eq}) of the globular microstructure with variation in the holding time of the final step. The equivalent diameter is the highest in case of t_{h3} = 1 min (i.e., 130 μm), and then decreases with increasing t_{h3}. The minimum mean equivalent diameter of the solid grains was 92 μm under the condition t_{h3} = 4 min. On the whole, the result of the 319 alloy was very similar to that of the 357 alloy in terms of the tendency of the microstructure to change size with variations in reheating conditions. However, through investigation of the equivalent diameter, it is known that the rate of globularization and coarsening of the 319 alloy is slower than in the case of the 357 alloy, because the 357 alloy has a higher thermal conductivity than the 319 alloy.

In the induction reheating process, the main driving forces of heating are eddy current and hysteresis loss. However, during the holding step in the reheating process, the conduction phenomenon is a stronger heating factor than eddy current heating, because the heating rate (Q) of the induction heating system for the holding step is substantially lower than that of the heating step.

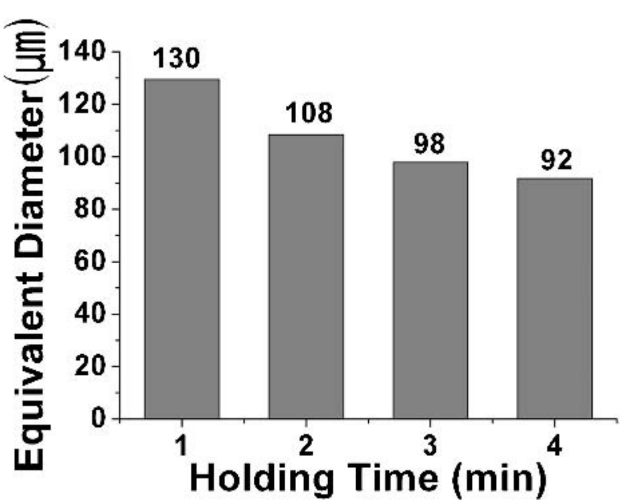

Fig. 13 Globule size of the 319 alloy with variation in the t_{h3}

Therefore, it is suggested that the rate of the microstructural change of the 357 alloy is faster than that of the 319 alloy, because the 357 alloy has a higher thermal solid conductivity than the 319 alloy. At 25 °C, the thermal conductivities of 319 and 357 Al are 109 W/m K and 151 W/m K, respectively.[15]

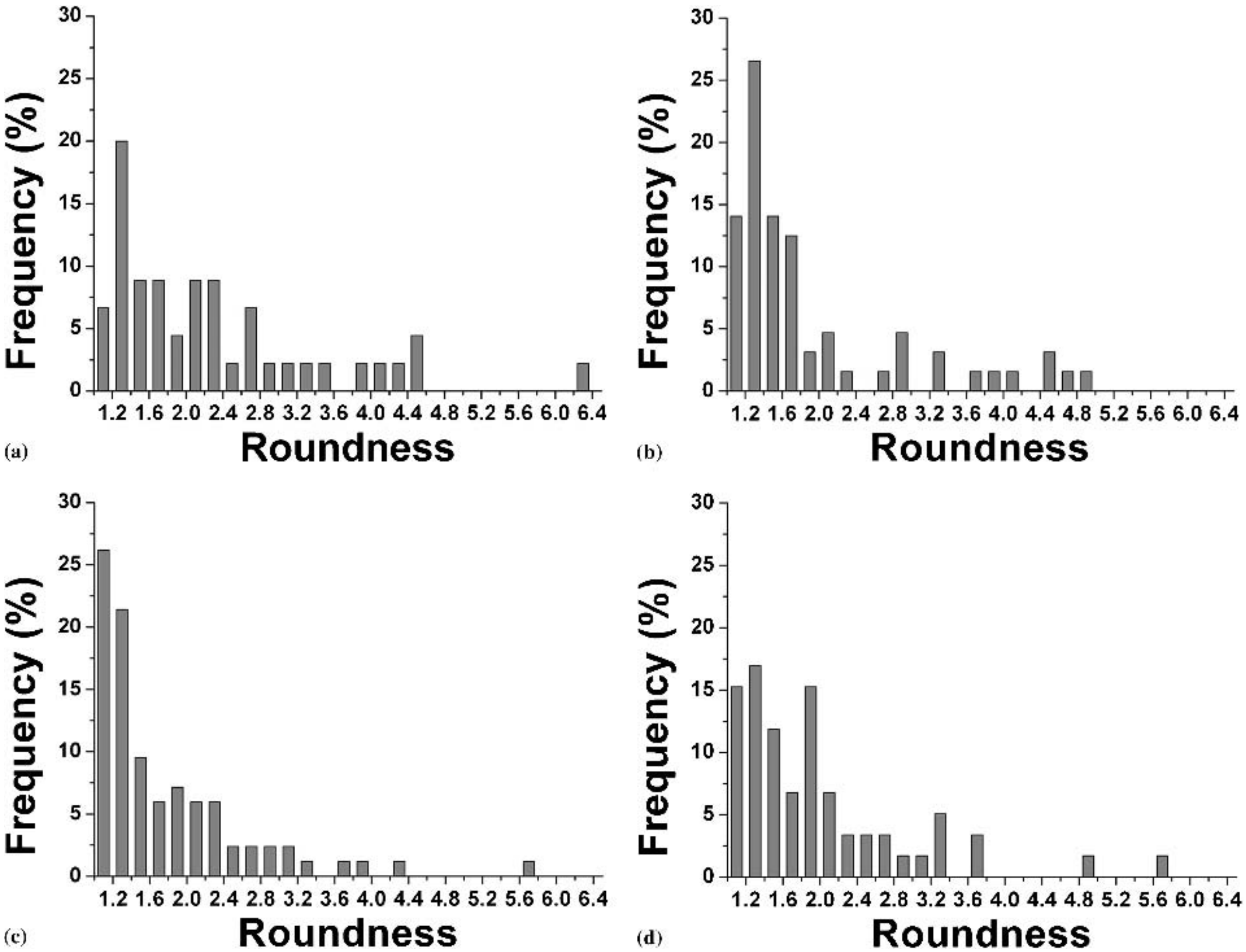

Fig. 14 Roundness of the 319 alloy with variation in the t_{h3}: **(a)** $t_{h3} = 1$ min; **(b)** $t_{h3} = 2$ min; **(c)** $t_{h3} = 3$ min; and **(d)** $t_{h3} = 4$ min

Figure 14 shows the R value for the 319 alloys with variations in the holding temperature of the final step (t_{h3}). In the case of $t_{h3} = 1$ min, the volume fractions of the solid grains with $1 \leq R \leq 1.2$ and $1 \leq R \leq 2$ are 6.7% and 48.9%, respectively. In the case of $t_{h3} = 2$ min, the volume fractions of the solid grains with $1 \leq R \leq 1.2$ and $1 \leq R \leq 2$ are 14.1% and 70.3%, respectively. In the case of $t_{h3} = 3$ min, the volume fractions of the solid grains with $1 \leq R \leq 1.2$ and $1 \leq R \leq 2$ are 26.2% and 70.2%, respectively. When $t_{h3} < 3$ min, the globularization phenomena of the solid grains increase with increasing holding time of the final reheating step (t_{h3}). However, when $t_{h3} = 4$ min, more improvement with respect to R was not observed because coalescence of the solid grains started to occur. In this case, the volume fractions of the solid grain with $1 \leq R \leq 1.2$ and $1 \leq R \leq 2$ are 15.3% and 66.1%, respectively.*

Figure 15 shows the microstructure of the A390 alloy with variation in the holding temperature of the final step (t_{h3}). It was observed that the microstructure of the hypereutectic A390 Al alloy shows a finer solid grain than that of the hypoeutectic alloys (i.e., 357 and 319 alloys) due to its higher Si content. During reheating, the solid grain growth is constrained by the Si particles. Therefore, it is observed that the microstructural change in the A390 alloy with increasing holding time of the final reheating step (t_{h3}) is not remarkable compared with that of the 357 or 319 alloy.

Figure 16 shows the equivalent diameter of the A390 alloy with variation in the holding temperature of the final step (t_{h3}). In this case, the remarkable variation of the equivalent diameter was not observed compared with the 319 and 357 alloys. When $t_{h3} = 2$ min, the solid grains with a minimum mean equivalent diameter of 61 μm were observed. Also, it is known that a remarkable change in the solid grain size with variation in t_{h3} did not occur.

Figure 17 shows the R distribution of the A390 alloy with variation in the holding temperature of the final step (t_{h3}). In the case of $t_{h3} = 1$ min, the volume fractions of the solid grains with $1 \leq R \leq 1.2$ and $1 \leq R \leq 2$ are 5.6% and 60.6%, respectively. In the case of $t_{h3} = 2$ min, the volume fractions of the solid grains with $1 \leq R \leq 1.2$ and $1 \leq R \leq 2$ are 11.2% and 75.0%, respectively. When $t_{h3} = 3$ min, the volume fractions of the solid grains with $1 \leq R \leq 1.2$ and $1 \leq R \leq 2$ are 15.0% and 75%, respectively. In case of $t_{h3} = 4$ min, the volume fractions of the solid grains with $1 \leq R \leq 1.2$ and $1 \leq R \leq 2$ are 14.3% and 77.1%, respectively. As shown in the cases of $t_{h3} = 2$, 3, and 4 min, the volume fractions of the solid

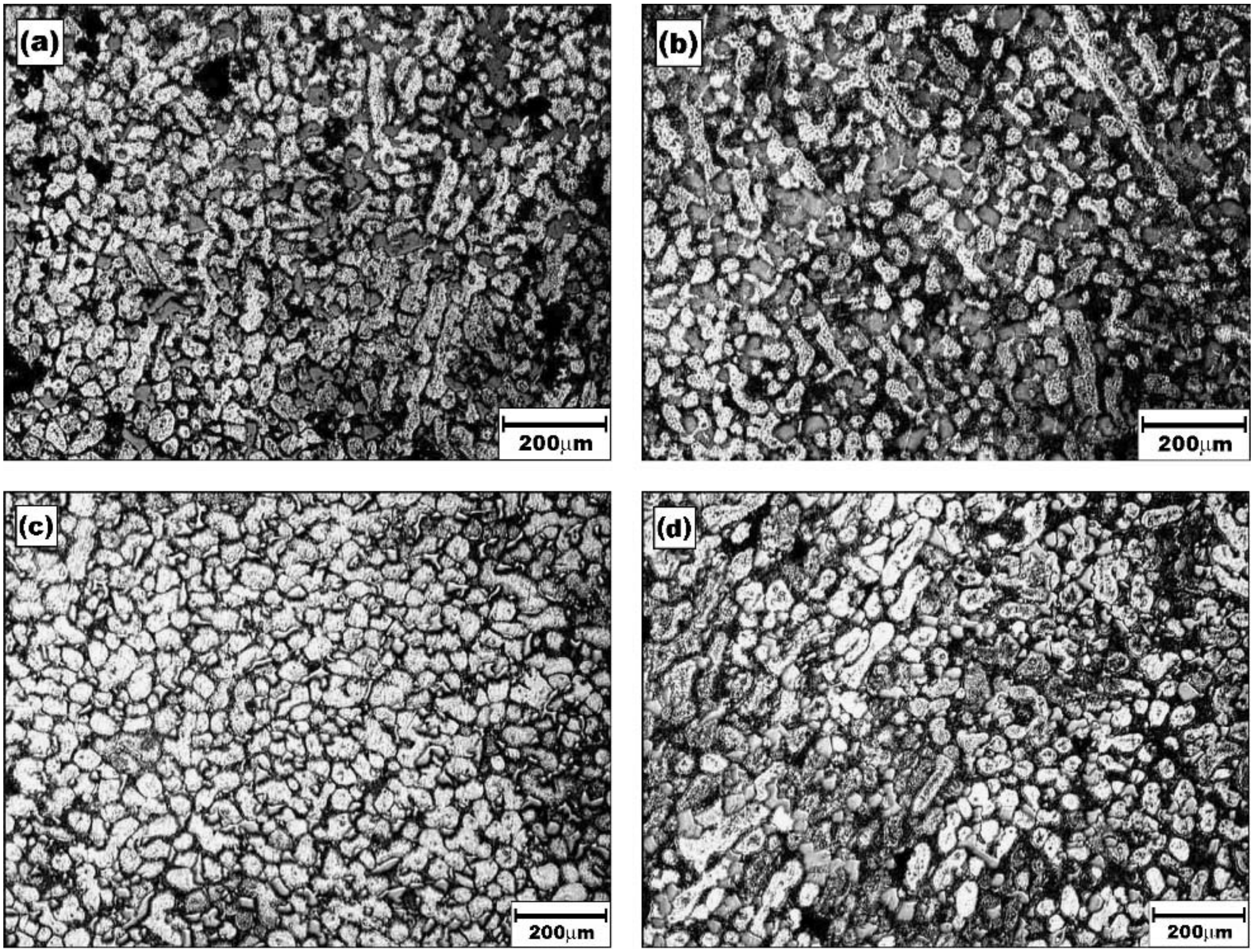

Fig. 15 Microstructure evolution of the A390 alloy with t_{h3} of **(a)** 1 min, **(b)** 2 min, **(c)** 3 min, and **(d)** 4 min

grains with $1 \leq R \leq 2$ show almost the same value. From these data, it is known that the change in R with variation in the reheating condition t_{h3} is not significant, because solid grain growth was constrained by the Si particles.

3.1.3 Effect of Holding Time of the Final Reheating Temperature on Mechanical Properties. To investigate the relationship between mechanical properties and globular microstructure size obtained by varying the holding time of the final reheating temperature (t_{h3}), tension tests were performed.

The reheating experiments were performed for variations in the holding time of the final reheating temperature (t_{h3}). The billets reheated under the conditions in Table 2 were quenched in water, and tensile test specimens extracted.

Figure 18 shows the relationship between the stress and strain for the 357 Al alloy after reheating. In the case of t_{h3} = 1 min, the ultimate strength and elongation showed relatively low values, 213 MPa and 2.2%, respectively.

As shown in Fig. 10, dendritic microstructures were observed because the globularization of the solid grains was incomplete due to the lack of holding time of the final reheating step (t_{h3}). In the t_{h3} range of 2-3 min, the maximum tensile strength and elongation were obtained because the globularization of the solid grains was completed. When t_{h3} is > 4 min, the ultimate tensile strength decreased due to the coarsening of the globular solid grains.

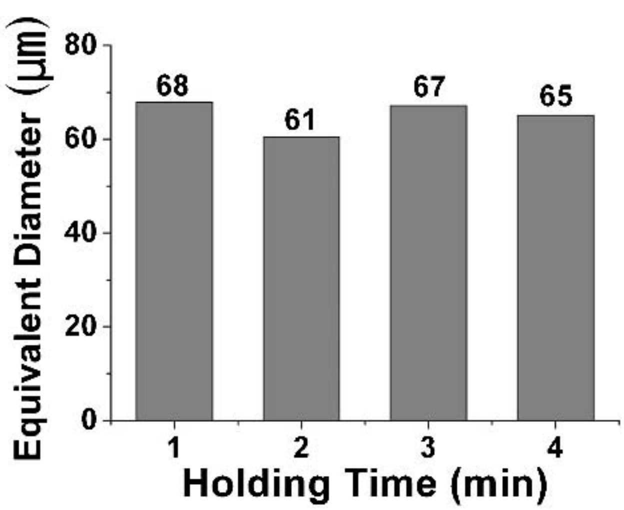

Fig. 16 Globule size of A390 alloy with variation in t_{h3}

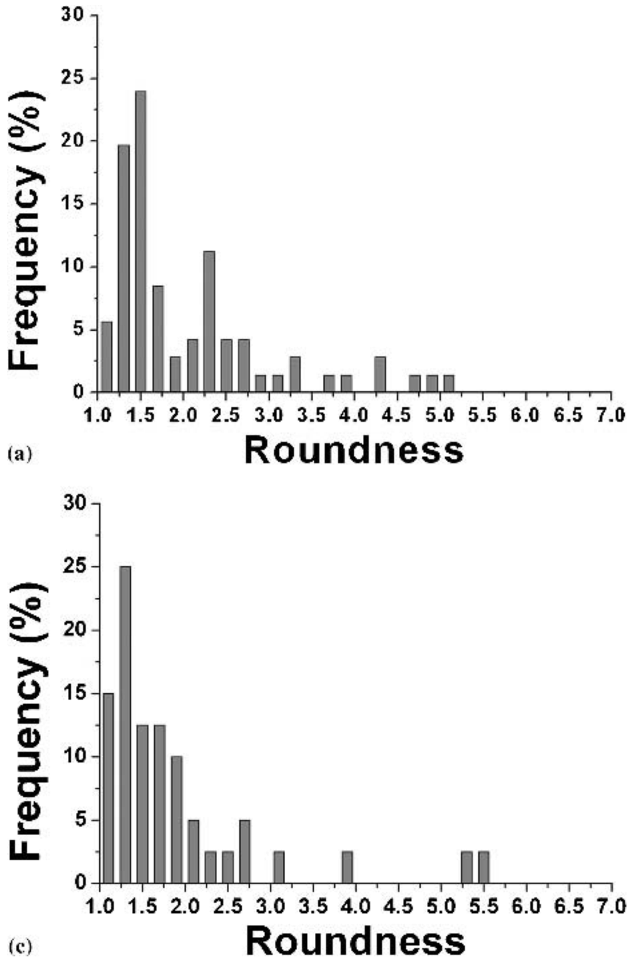

Fig. 17 Roundness of A390 alloy with variation in the t_{h3}: **(a)** $t_{h3} = 1$ min; **(b)** $t_{h3} = 2$ min; **(c)** $t_{h3} = 3$ min; and **(d)** $t_{h3} = 4$ min

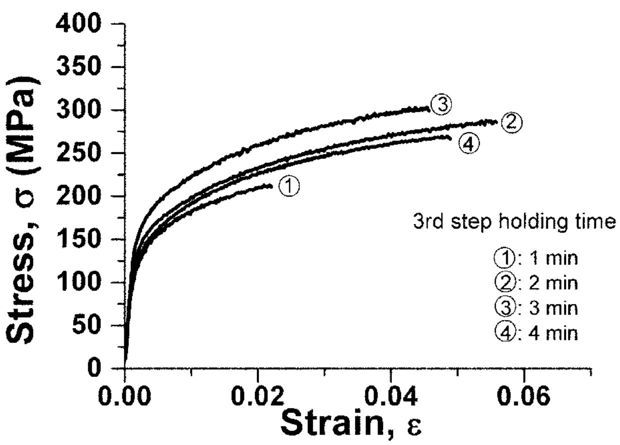

Fig. 18 Stress-strain curve of reheated 357 alloy

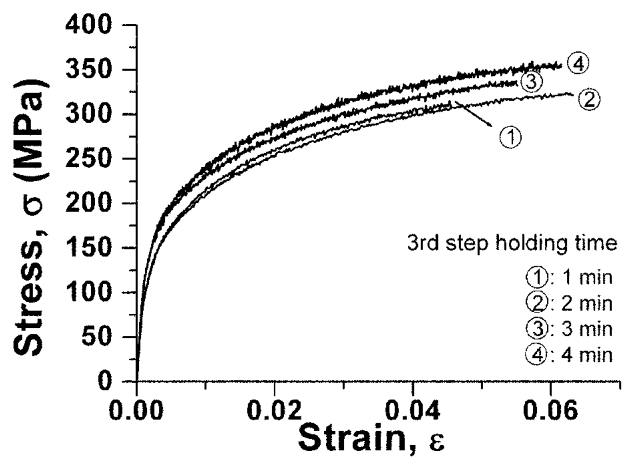

Fig. 19 Stress-strain curve of reheated 319 alloy

Figure 19 shows the relationship between the stress and strain of the 319 Al alloy after reheating. On the whole, ultimate tensile strength increased with increasing t_{h3}, and the maximum tensile strength was obtained in the case of $t_{h3} = 4$ min. Also, similar to the case of the 357 Al alloy, the minimum elongation was obtained under the reheating condition $t_{h3} = 1$ min. Considering that the tendency of the microstructure to change in a similar manner with variation in t_{h3}, it is predicted that the mechanical properties of the A390 alloy will decrease under the reheating condition $t_{h3} > 4$ min.

Figure 20 shows the stress-strain curves of A390 alloy after

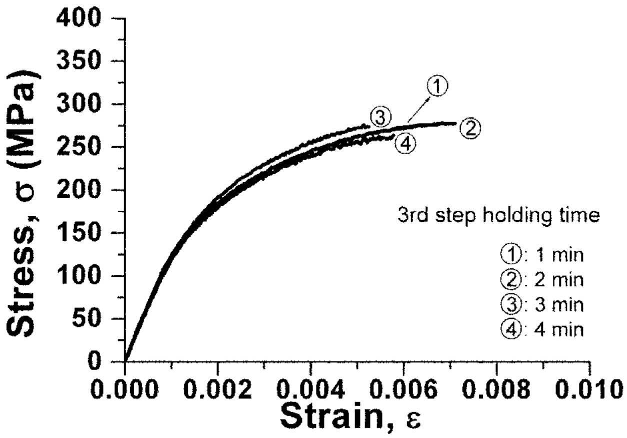

Fig. 20 Stress-strain curve of reheated A390 alloy

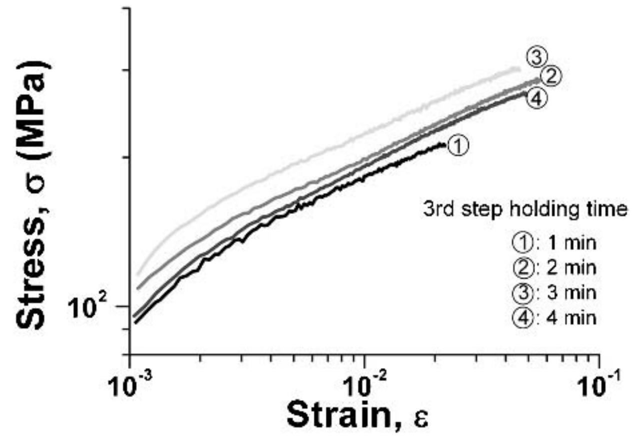

Fig. 21 Log-log strain-stress curve of reheated 357 alloy

reheating. The maximum ultimate tensile strength and the elongation were obtained for the reheating condition of $t_{h3} = 2$ min. However, the change of the mechanical properties with variation in the holding time of the final reheating temperature (t_{h3}) is not remarkable, and the maximum mechanical property values are much lower compared with the cases of 319 and 357 Al alloys. The reason for the minor change in the mechanical properties is that the growth of the solid grains was constrained by numerous Si particles within the eutectic. Also, it is reported that in the case of hypereutectic Al-Si alloys elongation rapidly decreases with increasing Si content, since silicon is hard and brittle.[16]

Table 3 shows the mechanical properties of the 357, 319, and A390 alloys with variations in the holding time of the final reheating step (t_{h3}).

3.1.4 Formulation of the Relationship Between Globular Solid Grain Size and Stress-Strain. For application to the design of a component using semi-solid forming, the relationship between globular solid grain size and stress-strain relation was formulated. The stress-strain relationship in the elastic deformation region can be described by Hooks law ($\sigma = K\varepsilon$), and that of the plastic deformation region can be described using the following power law relation (Eq 3):

$$\sigma = K\varepsilon^n \quad \text{(Eq 3)}$$

where σ, ε, K, and n are the stress, strain, strength coefficient, and strain-hardening exponent, respectively.

To obtain K and n, the σ-ε curve for each specimen was converted to a log σ-log ε plot.

Figures 21-23 show the relationship of stress to strain as represented by log ε versus log σ curve using the results of tension experiments using 357, 319, and A390 Al alloys. From the log ε-log σ curves, it is necessary to consider only the plastic deformation region. K and n values were obtained for variations of equivalent diameter, and these results are shown in Table 4.

As shown in Fig. 24, a linear fit using the least squares method was performed relating K to D_{eq}, that is, a flow stress equation was developed that accounts for the globular microstructure size of the semi-solid billet.

Table 3 Mechanical Properties for Variation of Holding Time (at RT)

Material	t_{h3}, min	Ultimate Tensile Strength, MPa	Yield Stress, MPa	Modulus of Elasticity, GPa	Elongation, %
357	1	213	143	98	2.2
	2	288	158	107	5.7
	3	303	180	101	4.7
	4	270	148	101	5.0
319	1	309	154	106	4.7
	2	324	153	98	6.5
	3	335	179	106	5.7
	4	353	185	110	6.3
A390	1	277	277	107	0.7
	2	278	278	115	0.8
	3	275	275	114	0.5
	4	263	263	115	0.6

However, in the current study, only four stress-strain curves for each material type were used to obtain the power law relation. Therefore, to obtain a more accurate power law relationship that can be applied to the thixoforging process, it is necessary to obtain more data.

4. Conclusions

Through an investigation of the microstructures and the mechanical properties with variation in the holding time of the final reheating step (t_{h3}), the following conclusions were reached:

1) Remarkable changes in the tensile strength and elongation of the 357 alloy were observed with variation in the holding time of the final reheating step. Under the reheating condition of $t_{h3} = 3$ min, the lowest equivalent globule diameter of 94 μm was obtained and the maximum ultimate tensile strength (303 MPa) was achieved.
2) Increasing the holding time of the final reheating step (t_{h3} = 1-4 min), the globular microstructure size and tensile

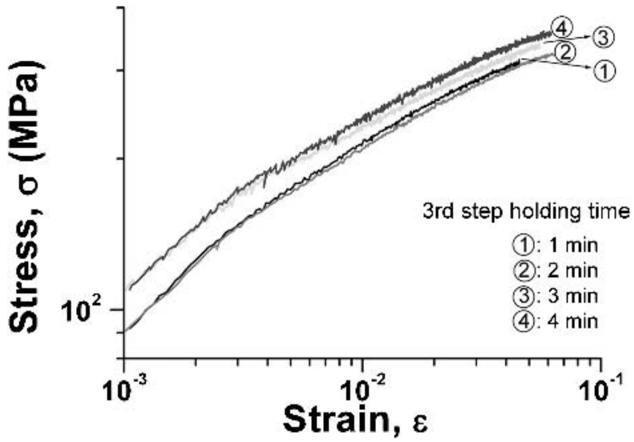

Fig. 22 Log-log strain-stress curve of reheated 319 alloy

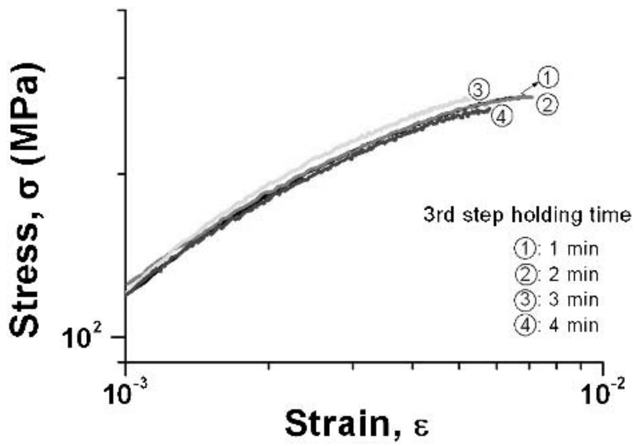

Fig. 23 Log-log strain-stress curve of reheated A390 alloy

Table 4 Strength Coefficient and Strain-Hardening Exponent for Variation of Equivalent Diameter (After Reheating)

357 Alloy			319 Alloy			A390 Alloy		
D_{eq}, μm	*K*, MPa	m	D_{eq}, μm	*K*, MPa	m	D_{eq}, μm	*K*, MPa	m
118	554	0.24	130	796	0.29	68	2328	0.41
110	559	0.23	108	719	0.27	61	2141	0.38
104	572	0.24	98	715	0.25	67	3194	0.46
94	598	0.22	92	754	0.25	65	2630	0.43

strength of the 319 Al alloy decreased and increased, respectively. Under the reheating condition of $t_{h3} = 4$ min, the lowest equivalent globule diameter, equal to 92 μm, and the maximum ultimate tensile strength, equal to 353 MPa, were achieved.

3) In the case of the hypereutectic A390 alloy, the lowest equivalent globule diameter of 61 μm and the maximum ultimate tensile strength (278 MPa) were achieved under the reheating condition of $t_{h3} = 2$ min. Also, it was observed that changes in the globular microstructure size and ultimate tensile strength and elongation with variation in t_{h3} were not remarkable compared with the hypoeutectic Al alloy due to the high Si content.
4) For the thixoforging process, the formulation of a stress-strain relationship that considers globular microstructure size as a variable was proposed, and a database for the thixoforging component design was established.

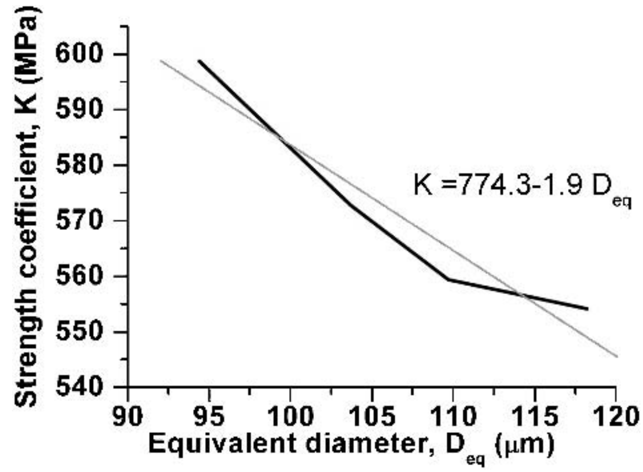

Fig. 24 Strength coefficient for variation of equivalent diameter (357 alloy)

Acknowledgments

This work was supported by the National Research Laboratory (NRL) program of the Korean Ministry of Science and Technology (KMOST). The authors would like to express their deep gratitude to the KMOST for financial assistance.

References

1. K.P. Young and R. Fitze: "Semi-Solid Metal Cast Aluminum Automotive Components" in *Proc. 3rd Int. Conf. on Semi-Solid Processing of Alloys and Composites*, M. Kiuchi, ed., Institute of Industrial Science, University of Tokyo, Tokyo Japan, 13-15 June 1994, pp. 155-76.
2. K. Kitamura, Y. Ando, K. Hironaka, S. Yahata, and C. Yoshida: "Die Casting of Aluminum Alloy in Semi-Solid State" in *Proc. 3rd Int. Conf. on Semi-Solid Processing of Alloys and Composites*, M. Kiuchi, ed., Institute of Industrial Science, University of Tokyo, Tokyo Japan, 13-15 June 1994, pp. 181-89.
3. T. Witulski, A. Winkelman, and G. Hirt: "Thixoforming of Aluminum Components for Lightweight Structure" in *Proc. 4th Int. Conf. on Semi-Solid Processing of Alloys and Composites*, D. H. Kirkwood and P. Kapranos, ed., University of Sheffield, Sheffield, UK, 19-21 June 1996, pp. 242-47.
4. W.L. Winterbottom: "Semi-Solid Forming Applications: High Volume Automotive Products" in *Proc. 6th Int. Conf. on Semi-Solid Processing of Alloys and Composites*, Turin, Italy, Sep., G. L. Chiarmetta and M. Rosso, ed., 27-29 Sept 2000, pp. 73-78.
5. C.G. Kang, H.K. Jung, and Y.J. Jung: "Coil Design of Induction Heating and Reheating Process of Aluminum Alloys for Thixoforming" in *Advanced Technology of Plasticity*, M. Geiger, ed., 3, Springer-Verlag, Germany, 1999, pp. 1689-94.
6. H.K. Jung and C.G. Kang: "Reheating Process of Cast and Wrought Aluminum Alloys for Thixoforming and Their Globularization Mechanism," *J. Mater. Proc. Technol.*, 2000, *104*, pp. 244-53.
7. S. Midson, V. Rudnev, and R. Gallik: "The Induction Heating of

Semi-Solid Aluminum Alloys" in *Proc. 5th Int. Conf. on Semi-Solid Processing of Alloys and Composites*," Golden, CO, June, A.K. Bhasin, J.J. Moore, K.P. Young, and S. Midson, ed., Colorado School of Mines, Golden, CO, 23-25 June 1998, pp. 497-504.

8. W.R. Lou, M. Brimont, C. Pluchon, P.Y. Menet, and M. Garat: "Metallurgical Aspects of Thixoforming of A356.0 and 357.0 Alloys," NADCA Transactions, Indianapolis, IN, 1995, pp. 389-96.
9. S. Sannes, H. Gjestland, L. Arnberg, and J.K. Solberg: "Microstructure Coarsening of Semi-Solid Mg Alloys" in *Proc. 3rd Int. Conf. on Semi-Solid Processing of Alloys and Composites*, Tokyo, June, M. Kiuchi, ed., Institute of Industrial Science, University of Tokyo, Tokyo, Japan, 13-15 June 1994, pp. 75-84.
10. N. Wang, J. Wu, and G. Shu: "Tensile and Compression Properties of Stircast Al-5%Cu and Al-80%Zn" in *Proc. 3rd Int. Conf. on Semi-Solid Processing of Alloys and Composites*, Tokyo, June, M. Kiuchi, ed., Institute of Industrial Science, University of Tokyo, Tokyo, Japan, 13-15 June 1994, pp. 127-34.
11. M. Ferrante and E. de Fretias: "Rheology and Microstructural Development of a Al-4wt%Cu Alloy in the Semi-Solid State," *Mater. Sci. Eng.*, 1999, *A271*, pp. 172-80.
12. H.K. Jung and C.G. Kang: "A Study on Induction Heating Process of Al-6%Si-3%Cu-0.3Mg Alloy for Thixoforming," *J. Korean Foundrymen's Soc.*, 1999, *19*(3), pp. 25-35.
13. H.K. Jung and C.G. Kang: "An Induction Heating Process with Coil Design and Solutions Avoiding Coarsening Phenomena of Al-6 Pct Si-3 Pct Cu-0.3 Pct Mg Alloy for Thixoforming," *Metall. Trans. A*, 1999, *30A*, pp. 2967-77.
14. J.A. Danzig, S.P. Midson: "Billet Heating for Semi-Solid Forming" in *Proc. 2nd Int. Conf. on the Semi-Solid Processing of Alloys and Composites*," Massachusetts Institute of Technology, Cambridge, MA, 10-12 June, S.B. Brown and M.C. Flemings, ed., 1992, pp. 105-18.
15. American Society for Metals: *Metals Handbook – Vol 2: Properties and Selection: Nonferrous Alloys and Special-purpose Materials*, ASM International, Metals Park, OH, 1990.
16. R.M. Brick, A.W. Pense, and R.B. Gordon: *Structure and Properties of Engineering Materials*, 4th ed., McGraw-Hill Book Company, New York, 1977, pp. 186-87.